



# Upper-Convected Maxwell Fluid Flow with Variable Thermo-Physical Properties over a Melting Surface Situated in Hot Environment Subject to Thermal Stratification

A. J. Omowaye and I. L. Animasaun<sup>†</sup>

*Department of Mathematical Sciences,  
 Federal University of Technology, Akure, Ondo State, Nigeria, West Africa.*

*Corresponding Author Email: anizakph2007@gmail.com*

(Received April, 21, 2015; accepted August, 2, 2015)

## ABSTRACT

An upper-convected Maxwell (UCM) fluid flow over a melting surface situated in hot environment is studied. The influence of melting heat transfer and thermal stratification are properly accounted for by modifying the classical boundary condition of temperature to account for both. It is assumed that the ratio of inertia forces to viscous forces is high enough for boundary layer approximation to be valid. The corresponding influence of exponentially space dependent internal heat generation on viscosity and thermal conductivity of UCM is properly considered. The dynamic viscosity and thermal conductivity of UCM are temperature dependent. Classical temperature dependent viscosity and thermal conductivity models are modified to suit the case of both melting heat transfer and thermal stratification. The governing non-linear partial differential equations describing the problem are reduced to a system of nonlinear ordinary differential equations using similarity transformations and completed the solution numerically using the Runge-Kutta method along with shooting technique (RK4SM). The numerical procedure is validated by comparing the solutions of RK4SM with that of MATLAB based bvp4c. The results reveal that increase in stratification parameter corresponds to decrease in the heat energy entering into the fluid domain from freestream and this significantly reduces the overall temperature and temperature gradient of UCM fluid as it flows over a melting surface. The transverse velocity, longitudinal velocity and temperature of UCM are increasing function of temperature dependent viscous and thermal conductivity parameters. At a constant value of melting parameter, the local skin-friction coefficient and heat transfer rate increases with an increase in Deborah number.

**Keywords:** Melting heat transfer; Viscoelastic fluid; Relaxation time; Variable viscosity; Variable thermal conductivity; Thermal Stratification; Exponentially Internal heat Source.

## NOMENCLATURE

$a$	stretching rate (S.I. Unit $second^{-1}$ )	$T$	dimensional fluid temperature
$b_1$	temperature dependent viscous parameter	$T_m$	melting temperature
$b_2$	temperature dependent thermal conductivity parameter	$T_\infty$	ambient temperature
$B_o$	uniform magnetic field	$u$	velocity component along horizontal surface
$C_f$	skin friction coefficient	$v$	velocity component along vertical surface
$C_p$	specific heat at constant pressure	$x$	distance along horizontal surface
$d_{ij}$	deformation rate tensor	$y$	distance along vertical surface
$L_{ij}$	velocity gradient tensor		
$M$	magnetic parameter	$\beta$	Deborah number (dimensionless viscoelastic parameter)
$N_{ux}$	local Nusselt number	$\gamma$	space dependent heat source parameter
$P_r$	Prandtl number		
$q_w$	heat transfer		

$\varepsilon$	dimensionless temperature dependent thermal conductivity parameter	$\xi$	dimensionless temperature dependent viscous parameter
$\eta$	similarity variable	$\rho$	density of UCM fluid
$\theta$	dimensionless temperature	$\sigma$	electric conductivity
$\vartheta$	kinematics viscosity	$\tau_{ij}$	tensor notation
$\kappa$	thermal conductivity	$\tau_w$	skin friction
$\lambda$	dimensional relaxation time	$\Psi$	stream function
$\mu$	dynamic viscosity of UCM fluid		

### 1. INTRODUCTION

The analysis and description of boundary layer flow together with heat transfer of an incompressible fluid on a stretching horizontal surface has gained attention of many researchers. Series of investigations have been carried out towards the understanding of the dynamics of viscoelastic material since the contribution of James Clerk Maxwell in 1867 to the body of knowledge. The dynamics of material having the properties of elasticity and viscosity when undergoing deformation is a fundamental topic in fluid dynamics. This kind of material referred to as Maxwell fluid has attracted the attention of many researchers due to its wide industrial and technical applications. The upper-convected Maxwell model can be described as the generalization of the Maxwell material for the case of large deformation using the upper-convected time derivative (also known as Oldroyd derivative) which is the rate of change of some tensor property of a small parcel of fluid that is written in the coordinate system stretching with the fluid. It is worth noticing that mathematical model of upper-convected Maxwell has been described (or defined) as a function of stress tensor, relaxation time, upper convected time derivative of stress tensor, fluid velocity, material viscosity at steady simple shear and tensor of the deformation rate.

It is a common known fact in rheology that given enough time, even a solid-like material will flow Barnes *et al.* (1989). In view of this, a dimensionless number that incorporates both the elasticity and viscosity of material is required. Poole (2012) reported the history behind the given name "Deborah" and further explained Deborah number as the ratio of time it takes for a material to adjust to deformations according to Eugene C. Bingham and Markus Reiner. In view of this, Sadeghy *et al.* (2005) investigated Sakiadis flow of a UCM fluid. The role played by a fluid's elasticity on the characteristics of its Sakiadis flow was analyzed. In the same context, it was reported that at high Deborah number, UCM flow corresponds to

solid-like behavior and low Deborah numbers to fluid-like behavior. Recently, Shateyi *et al.* (2015) investigated entropy generation on a magnetohydrodynamic flow and heat transfer of a Maxwell fluid over a stretching sheet in a Darcian porous medium. In the research, a new numerical scheme (Chebyshev spectral collocation method) was adopted to solve the nonlinear systems of boundary value problem.

Considering some rheological complex fluids such as polymer solutions, blood, ice creams and synovia fluid, Abbas *et al.* (2006) argued that the second-grade fluid model adopted in the work of Fosdick and Rajagopal (1979) does not give reasonable results for flows of highly elastic fluids (polymer melts) that occur at high Deborah number. For such situations the upper-convected Maxwell (UCM) model is quite appropriate. Using the UCM model, MHD boundary layer flow of a UCM fluid in a rectangular porous channel was successfully investigated. The study on dynamics of upper-convected Maxwell fluid is extended in Hayat *et al.* (2006) and reported that boundary layer thickness decreases by increasing the magnitude of MHD parameter, suction/injection velocity parameter and relaxation time parameter. In recent years, many researchers has investigated and reported the effect of some parameters on upper-convected Maxwell fluid flow (see Sadeghy *et al.* (2006), Abbas *et al.* (2008), Sadeghy *et al.* (2009), Pop *et al.* (2012), Motsa *et al.* (2012), Mustafa *et al.* (2012), Prasad *et al.* (2013) and Animasaun *et al.* (2015)).

Internal energy generation can be explained as a scientific method of generating heat energy within a body by chemical, electrical or nuclear process. Natural convection induced by internal heat generation is a common phenomenon in nature. Crepeau and Clarksean (1997) have reported a similarity solution of a fluid problem along a vertical plate with constant temperature in the presence of an exponential decaying heat generation term under the assumption that the fluid has an internal volumetric heat generation.

In many situations, there may be appreciable temperature difference between the surface and the ambient fluid. This necessitates the consideration of temperature dependent heat source(s) that may exert a strong influence on the heat transfer characteristics (see Salem and El-Aziz (2007)). Salem and El-Aziz (2008) further stated that exact modeling of internal heat generation or absorption is quite difficult and argued that some simple mathematical models can express its average behavior for most physical situations. Recently, Animasaun *et al.* (2015) reported that when the plastic dynamic viscosity and thermal conductivity of non-Newtonian Casson fluid are considered as temperature dependent, exponentially decaying internal heat generation parameter is an important dimensionless number that can be used to increase velocity and temperature of the fluid as it flows.

Effect of this internally generated heat energy on the surface may lead to melting of solid surface. From the knowledge of kinetic theory of matter, some solids may melt if expose to a high temperature. In an earlier study, the effect of melting on heat transfer was studied by Yin-Chao and Tien (1963) for the Leveque problem. The tangential velocity profile is assumed to be linear. It was further reported by Tien and Yen (1965) that the approximation in Yin-Chao and Tien (1963) is valid if one deals with a high Prandtl number fluid so that the significant temperature change takes place only within a thin layer of fluid immediately adjacent to the solid boundary and consequently the velocity profile inside this thin layer can be approximated by a linear segment. In addition, effect of melting on heat transfer between melting body and surrounding fluid qualitatively from the point of view of boundary layer theory was investigated. This contribution to the existing knowledge attracted Epstein (1975) to present a note on a systematic method of calculating steady state melting rates in all circumstances involving the melting of solid bodies immersed in streams of warmer fluid of the same material. In the same context, relationship between boundary condition of evaporation and that of melting is discussed. In recent years, many researchers have investigated and reported the effect of melting parameters; for details see Pop *et al.* (2010), Ishak *et al.* (2010) and Hayat *et al.* (2013).

In all of the above mentioned studies, fluid viscosity and thermal conductivity have been assumed to be constant function of temperature

within the boundary layer. However, it is known that physical properties of the fluid may change significantly when expose to internal generated temperature. For lubricating fluids, heat generated by the internal friction and the corresponding rise in temperature affect the viscosity of UCM and so the viscosity of UCM can no longer be assumed constant. In a case of melting as reported by many researchers (i.e. Fukusako and Yamada (1999), Pop *et al.* (2010), Ishak *et al.* (2010), Hayat *et al.* (2013)), it is worth mentioning that temperature of fluid layers at free stream may also have significant effect on the intermolecular forces of upper convected Maxwell fluid. The increase of temperature may also leads to a local increase in the transport phenomena by reducing the viscosity across the momentum boundary layer and so the heat transfer rate at the wall may also be affected greatly.

According to Batchelor (1987), Animasaun (2015a) and Meyers *et al.* (2006), it is a well-known fact that properties which are most sensitive to temperature rise are viscosity and thermal conductivity. Recently, Mukhopadhyay (2013) considered this same fact in order to explain stagnation point flow behavior on non-melting surface. Motivated by all the works mentioned above, it is of interest to contribute to the body of knowledge by studying the dynamics of upper-convected Maxwell fluid flow considering a case in which the influence of temperature on viscosity and thermal conductivity is properly accounted for. In this study we aim at investigating UCM fluid flow along a melting surface situated in hot environment which subjects the flow to thermal stratification. This is achieved by modifying and incorporating all the necessary term(s) into the boundary layer equation in line with boundary layer theory and heat transfer theory. Also, to unravel effects of corresponding parameters on the physical quantities of UCM fluid flow with variable thermo-physical properties towards hot environment. Lastly, to complements the research of Hayat *et al.* (2013), Mustafa *et al.* (2012), Pop *et al.* (2010), and Prasad *et al.* (2013).

It is evident that the results obtained from the present investigation will provide useful information for various industrial applications. In this paper, in section 2 we presents the mathematical formulation of the problem, in section 3 the numerical solution is presented, in section 4 the results and discussions are explained and in section 5 we presents the

conclusions based on the findings.

## 2. MATHEMATICAL FORMULATION

We consider steady and incompressible upper-convected Maxwell (UCM) fluid flow with variable thermo-physical properties along a melting surface situated in a hot environment. The flow under consideration is assumed to occupy the domain  $0 \leq y < \infty$  as shown in the Fig. 1. Boundary layer equations which best describe upper convected Maxwell fluid flow can be derived starting from Cauchy equations of motion. Following (Dunn and Rajagopal (1995) and

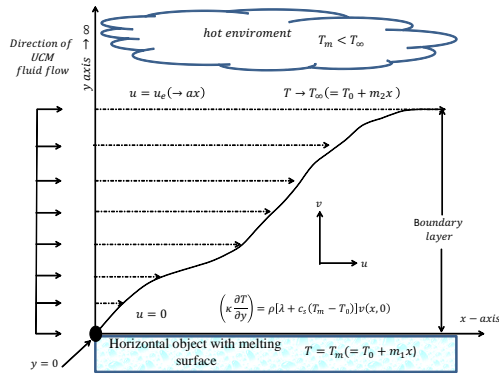


**Fig. 1. Physical Configuration.**

Sadeghy *et al.* (2005)), steady two-dimensional fluid flow can be written as

$$\frac{\partial u}{\partial x} + \frac{\partial v}{\partial y} = 0, \quad (1)$$

$$u \frac{\partial u}{\partial x} + v \frac{\partial u}{\partial y} = -\frac{1}{\rho} \frac{\partial p}{\partial x} + \frac{1}{\rho} \left( \frac{\partial \tau_{xx}}{\partial x} + \frac{\partial \tau_{xy}}{\partial y} \right), \quad (2)$$

$$u \frac{\partial v}{\partial x} + v \frac{\partial v}{\partial y} = -\frac{1}{\rho} \frac{\partial p}{\partial y} + \frac{1}{\rho} \left( \frac{\partial \tau_{yx}}{\partial x} + \frac{\partial \tau_{yy}}{\partial y} \right). \quad (3)$$

Where  $\rho$  is the density of the steady upper-convected Maxwell fluid. Poole (2012) explained that in steady simple shear flow (SSSF), the dominant elastic force will be due to the first normal-stress difference ( $\tau_{xx}$ ,  $\tau_{yy}$ ) and the viscous force is simply the shear stress ( $\tau_{xy}$ ). In Eq. (2) and Eq. (3), elastic terms are  $\frac{\partial \tau_{xx}}{\partial x}$  and  $\frac{\partial \tau_{yy}}{\partial y}$ . The viscous terms are  $\frac{\partial \tau_{xy}}{\partial y}$  and  $\frac{\partial \tau_{yx}}{\partial x}$ . Using order of magnitude as introduced by Ludwig Prandtl and stated in Schlichting (1964), it is valid to say that

$$u = O(1), \quad v = O(\delta), \quad x = O(1), \quad y = O(\delta), \quad (4)$$

and easy to show that in Eqs. (2) and (3), order of magnitude of the two elastic terms and order

of magnitude of the two viscous terms are the same if

$$\frac{\tau_{xx}}{\rho} = O(1), \quad \frac{\tau_{xy}}{\rho} = O(\delta), \quad \frac{\tau_{yy}}{\rho} = O(\delta^2). \quad (5)$$

This condition can be found in Sadeghy *et al.* (2005). Elastic effects should be considered in a boundary layer only for those viscoelastic fluids for which  $\tau_{xx}$  is of an order larger than  $\tau_{xy}$  and  $\tau_{yy}$ . Not all viscoelastic fluid models can meet such a strong restrictive condition. Assuming that a fluid can be found for which the order estimates as given by Eq. (5) really hold; the stress components of a UCM fluid can indeed be represented by the above order estimates justifying the use of such a model in the present work. The equations of motions can be simplified to

$$u \frac{\partial u}{\partial x} + v \frac{\partial u}{\partial y} = -\frac{1}{\rho} \frac{\partial p}{\partial x} + \frac{1}{\rho} \left( \frac{\partial \tau_{xx}}{\partial x} + \frac{\partial \tau_{xy}}{\partial y} \right), \quad (6)$$

$$0 + 0 = -\frac{1}{\rho} \frac{\partial p}{\partial y} + \frac{1}{\rho} (0 + 0). \quad (7)$$

In the presence of pressure gradient, the equations of motions together with continuity equation can be written as

$$\frac{\partial u}{\partial x} + \frac{\partial v}{\partial y} = 0, \quad (8)$$

$$u \frac{\partial u}{\partial x} + v \frac{\partial u}{\partial y} = -\frac{1}{\rho} \frac{\partial p}{\partial x} + \frac{1}{\rho} \left( \frac{\partial \tau_{xx}}{\partial x} + \frac{\partial \tau_{xy}}{\partial y} \right), \quad (9)$$

In Eq. (8) and Eq. (9), there exist five dependent variables which are  $p$ ,  $u$ ,  $v$ ,  $\tau_{xx}$  and  $\tau_{xy}$ . In order to resolve this (i.e. to make the number of unknowns equal to the number of equations), a constitutive equation relating stress components to the deformation field is needed. For a Maxwell fluid, the stress tensor ( $\tau_{ij}$ ) can be related to the deformation-rate tensor ( $d_{ij}$ ) as presented in Larson (1988) and Sadeghy *et al.* (2005) as

$$\left( \tau_{ij} + \lambda \frac{\Delta \tau_{ij}}{\Delta t} \right) = 2\mu^c d_{ij} \quad (10)$$

The time derivative ( $\frac{\Delta}{\Delta t}$ ) appearing in Eq. (10) is the so-called upper-convected time derivative which has been devised to satisfy the requirements of continuum mechanics (i.e. material objectivity and frame indifference; see Larson (1988) and Sadeghy *et al.* (2005)). In this paper, the zero-shear rate viscosity is denoted as  $\mu^c$ .

$$\frac{\Delta \tau_{ij}}{\Delta t} = \frac{D\tau_{ij}}{Dt} - L_{jk}\tau_{ik} - L_{ik}\tau_{kj} \quad (11)$$

In Eq. (11),  $L_{ij}$  is the velocity gradient tensor. The Bernoulli equation for the free stream flow just above the boundary layer where there is no viscous shear,

$$\frac{p}{\rho} + \frac{u_e^2}{2} = \text{constant}$$

can be differentiated and used to eliminate the pressure gradient Lienhard-IV and Lienhard-V (2008)

$$-\frac{1}{\rho} \frac{\partial p}{\partial x} = u_e \frac{\partial u_e}{\partial x}$$

Since the flow is along flat horizontal melting plate, pressure  $p$  and stretching velocity at the free stream  $u_e$  are constant; hence  $u_e \frac{\partial u_e}{\partial x}$  vanishes from the momentum equation. For an incompressible fluid obeying upper convected Maxwell model, the  $x$ -momentum equation can be simplified using the usual boundary layer theory approximations and then obtain

$$u \frac{\partial u}{\partial x} + v \frac{\partial u}{\partial y} + \lambda \left( u^2 \frac{\partial^2 u}{\partial x^2} + v^2 \frac{\partial^2 u}{\partial y^2} + 2uv \frac{\partial^2 u}{\partial x \partial y} \right) = \frac{\mu}{\rho} \frac{\partial^2 u}{\partial y^2} - \frac{\sigma B^2}{\rho} \left( u + \lambda v \frac{\partial u}{\partial y} \right) \quad (12)$$

In this study on Maxwell fluid flow, it is assumed that the normal stress is of the same order of magnitude as that of the shear stress in addition to the usual boundary layer approximation for deriving the component of the momentum boundary layer Eq. (12). This is properly accounted for by introducing  $\frac{\sigma B^2}{\rho} \left( \lambda v \frac{\partial u}{\partial y} \right)$  into the momentum Eq. (12). In this present study, it is important to state that exponential heat source is adopted to account for internal distribution of temperature in energy equation. This concept can be traced to the idea of Crepeau and Clarksean (1997), Salem and El-Aziz (2007), Salem and El-Aziz (2008), Reddy and Reddy (2011) and Animasaun *et al.* (2015). The energy equation can be written as

$$u \frac{\partial T}{\partial x} + v \frac{\partial T}{\partial y} = \frac{\kappa}{\rho C_p} \frac{\partial^2 T}{\partial y^2} + \frac{Q_o(T_\infty - T_o)}{\rho C_p} e^{(-ny\sqrt{\frac{\sigma}{\eta}})} \quad (13)$$

Equations (8), (12) and (13) are subject to the following boundary conditions

$$u = 0, \quad \kappa \left( \frac{\partial T}{\partial y} \right) = \rho [\lambda^* + c_s(T_m - T_o^*)]v(x, 0),$$

$$T = T_m, \quad \text{at } y = 0, \quad (14)$$

$$u \rightarrow ax, \quad T \rightarrow T_\infty, \quad \text{as } y \rightarrow \infty. \quad (15)$$

$\kappa$  is the thermal conductivity,  $\lambda^*$  is the latent heat of the fluid and  $c_s$  is the heat capacity of the solid surface. In order to solve the problem completely in unbounded domains, it is possible to augment the boundary conditions by assuming certain asymptotic structures for the solutions at infinity. The formulation of the second term in boundary Eq. (14) states that the heat conducted to the melting surface is equal to the heat of melting plus the sensible heat required to raise the solid temperature  $T_o^*$  to its melting temperature  $T_m$  (for details, see Epstein and Cho (1976)). The increase of temperature may also leads to a local increase in the transport phenomena by reducing the viscosity across the momentum boundary layer and so the heat transfer rate at the wall may also be affected greatly. Due to this, it is very important to account for the influence of temperature on the thermo-physical properties of UCM fluid as it flows over a melting surface within the boundary layer. However, it is known that physical properties of the fluid may change significantly when expose to space dependent internal generated temperature. For lubricating fluids, heat generated by the internal friction and the corresponding rise in temperature affect the viscosity of the fluid and so the fluid viscosity can no longer be assumed constant. In order to account for the variation in thermo-physical properties of the fluid as it flows past a horizontal melting surface, it is valid to consider the mathematical model of temperature dependent viscosity model used in Animasaun (2015b) and Sivagnana *et al.* (2009) which was developed using the experimental data of Batchelor (1987) together with the mathematical model of temperature dependent thermal conductivity model of Charraudeau (1975) as

$$\mu(T) = \mu^* [a_1 + b_1(T_w - T)],$$

$$\kappa(T) = \kappa^* [a_2 + b_2(T - T_\infty)], \quad (16)$$

These mathematical models together with classical similarity variables for temperature are modified to

$$\mu(T) = \mu^* [a_1 + b_1(T_\infty - T)], \quad \theta = \frac{T - T_m}{T_\infty - T_o},$$

$$\kappa(T) = \kappa^* [a_2 + b_2(T - T_m)] \quad (17)$$

From these equations, it is valid to say that

$$T_\infty - T = (1 - \theta)(T_\infty - T_o) - m_1 x$$

In this study, the idea of Animasaun (2015a) and Vimala and Loganathan (2015) is followed to define thermal stratification  $T_m$  at the melting wall ( $y = 0$ ) and at the free stream ( $T_\infty$ ) are defined as

$$T_m = T_o + m_1x, \quad T_\infty = T_o + m_2x. \quad (18)$$

From these models, the following relations can be easily deduced

$$b_1(T_m - T_o) = b_1m_1x, \quad b_1(T_\infty - T_o) = b_1m_2x. \quad (19)$$

$T_o$  is known as reference temperature. It is worth noticing from Eq. (19) that there exist two differences in temperature due to stratification that occur across the UCM fluid as it flows over a melting surface. These proposed models implies that effect of temperature on (i) the viscosity of UCM at the melting wall (ii) the viscosity of UCM at the free stream may be investigated separately. In view of this, it is valid to define temperature dependent viscous parameter  $\xi$  as first term in Eq. (20). The ratio of the two terms can thus produce the dimensionless stratification  $S_t$  parameter

$$\xi = b_1(T_\infty - T_o), \quad b_1(T_m - T_o) = \xi S_t, \quad S_t = \frac{m_1}{m_2} \quad (20)$$

Upon using Eq. (17) - Eq. (20), we obtain

$$u \frac{\partial u}{\partial x} + v \frac{\partial u}{\partial y} + \lambda \left( u^2 \frac{\partial^2 u}{\partial x^2} + v^2 \frac{\partial^2 u}{\partial y^2} + 2uv \frac{\partial^2 u}{\partial x \partial y} \right) =$$

$$\vartheta^* [a_1 + \xi - \theta \xi - \xi S_t] \frac{\partial^2 u}{\partial y^2} - \vartheta^* \xi \frac{\partial \theta}{\partial y} \frac{\partial u}{\partial y} - \frac{\sigma B^2}{\rho} \left( u + \lambda v \frac{\partial u}{\partial y} \right) \quad (21)$$

$$u \frac{\partial T}{\partial x} + v \frac{\partial T}{\partial y} = \frac{\kappa^* [a_2 + \theta \varepsilon] (T_\infty - T_o)}{\rho C_p} \frac{\partial^2 \theta}{\partial y^2}$$

$$+ \frac{\kappa^* b_2}{\rho C_p} (T_\infty - T_o)^2 \left( \frac{\partial \theta}{\partial y} \right)^2 + \frac{Q_o (T_\infty - T_o)}{\rho C_p} e^{(-ny\sqrt{\frac{a}{\vartheta}})} \quad (22)$$

In order to write the governing equations and the boundary conditions in dimensionless form, the following non-dimensional quantities are introduced,

$$v = -\frac{\partial \psi}{\partial x}, \quad u = \frac{\partial \psi}{\partial y}, \quad \eta = y\sqrt{\frac{a}{\vartheta}}, \quad \Psi = xf(\eta)\sqrt{a\vartheta}. \quad (23)$$

It is important to note that the first two terms of Eq. (23) automatically satisfy continuity Eq. (8). Then, Eq. (21) and Eq. (22) becomes

$$[a_1 + \xi - \theta \xi - \xi S_t - \beta f f] \frac{d^3 f}{d\eta^3} + \left( f - \xi \frac{d\theta}{d\eta} + 2\beta f \frac{df}{d\eta} + M\beta f \right) \frac{d^2 f}{d\eta^2} - \left( \frac{df}{d\eta} + M \right) \frac{df}{d\eta} = 0 \quad (24)$$

$$[a_2 + \varepsilon \theta] \frac{d^2 \theta}{d\eta^2} + \varepsilon \frac{d\theta}{d\eta} \frac{d\theta}{d\eta} - Pr S_t \frac{df}{d\eta} - Pr \theta \frac{df}{d\eta} + Pr f \frac{d\theta}{d\eta} + Pr \gamma e^{(-m\eta)} = 0 \quad (25)$$

The corresponding boundary conditions take the form

$$\frac{df}{d\eta} = 0, \quad m \frac{d\theta}{d\eta} + Pr f = 0, \quad \theta = 0 \quad \text{at} \quad \eta = 0 \quad (26)$$

$$\frac{df}{d\eta} \rightarrow 1, \quad \theta \rightarrow (1 - S_t) \quad \text{as} \quad \eta \rightarrow \infty \quad (27)$$

Here Deborah number  $\beta = \lambda a$ , temperature dependent thermal conductivity parameter  $\varepsilon = b_2(T_\infty - T_o)$ , Magnetic field parameter  $M = \frac{\sigma B^2}{a\rho}$ , Coefficient of thermal diffusivity  $\alpha = \frac{\kappa}{\rho C_p}$ , Prandtl number  $Pr = \frac{C_p \mu}{\kappa}$ , Heat source parameter  $\gamma = \frac{Q_o}{\rho C_p a}$  and melting parameter  $m = \frac{(T_\infty - T_o) C_p}{\lambda^* + c_s (T_m - T_o^*)}$ . The physical quantities of interest are the skin friction coefficient  $C_f$  and Local Nusselt number  $Nu_x$  which are defined by

$$C_f = \frac{\tau_w}{\rho (u_w)^2}, \quad Nu_x = \frac{aq_w}{\kappa (T_\infty - T_o)}$$

where the wall skin friction  $\tau_w$  and heat transfer from the surface  $q_w$  are

$$\tau_w = \left[ \mu \left( \frac{\partial u}{\partial y} \right) \Big|_{y=0} - \left( \lambda 2uv \frac{\partial u}{\partial x} + v^2 \frac{\partial u}{\partial y} \right) \Big|_{y=0} \right]$$

$$q_w = -\kappa \left( \frac{\partial T}{\partial y} \right) \Big|_{y=0}$$

Using variables Eq. (23)

$$Re_x^{1/2} C_f = \left( \frac{d^2 f}{d\eta^2} - \beta f f \frac{d^2 f}{d\eta^2} + 2\beta \frac{df}{d\eta} \frac{df}{d\eta} \right) \Big|_{\eta=0}$$

$$\frac{Nu_x}{Re_x^{1/2}} = - \left( \frac{\partial \theta}{\partial \eta} \right) \Big|_{\eta=0}, \quad Re_x^{1/2} = \frac{axx}{\vartheta}$$

the local Reynolds number is defined as  $Re_x^{1/2}$ .

### 3. METHOD OF SOLUTION

Numerical solutions of the ordinary differential equations Eq. (24) and Eq. (25) with the Neumann boundary conditions Eq. (26) and Eq. (27) are obtained using classical Runge-Kutta method with shooting. The BVP cannot be solved on an infinite interval, and it would be impractical to solve it for even a very large finite interval. In this work, we impose the infinite boundary condition at a finite point  $\eta_\infty = 6$ . The set of coupled ordinary differential equations along with boundary conditions have been reduced to a system of five simultaneous equations of first order for five unknowns following the method of superposition Na (1979). In order to integrate the corresponding I.V.P. the values of  $f(0)$ ,  $f''(0)$  and  $\theta'(0)$  are required, but no such values exist after the non-dimensionalization of the boundary conditions Eq. (14) and Eq. (15). It is important to report that, we may easily obtain  $f(0)$  by setting  $m = 0$ . The suitable guess values for  $G_1 = f''(0)$ ,  $G_2 = \theta'(0)$  and  $G_3 = f(0)$  are chosen and then integration is carried out. The condition is used as  $Guess = [(P_r G_3 + m G_2); 0; G_1; 0; G_2]$ . The calculated values for  $f(\eta)$  and  $\theta(\eta)$  at  $\eta = 6$  are compared with the given boundary conditions in Eq. (27) and the estimated values  $f(0)$ ,  $f''(0)$  and  $\theta'(0)$  are adjusted to give a better approximation of the solution. Series of values for  $f(0)$ ,  $f''(0)$  and  $\theta'(0)$  are considered and applied with fourth-order classical Runge-Kutta method using step size  $\Delta \eta = h = 0.01$ . The above procedure is repeated until asymptotically converged results are obtained within a tolerance level of  $10^{-4}$ . It is worth mentioning that there exist no related published articles that can be used to validate the accuracy of the numerical results. Eq. (24) - Eq. (27) can easily be solved using ODE solvers such as MATLAB's `bvp4c` solver (see Shampine *et al.* (2010)).

#### 3.1 Verification of the results

In order to verify the accuracy of the present analysis, the results of Classical Runge-Kutta together with shooting have been compared with that of `bvp4c` for the limiting cases when  $\xi = \varepsilon = \gamma = 0$ ,  $\beta = 0.3$ ,  $S_t = 0.3$ ,  $M = 0.5$  and  $n = 1$  at various values of  $P_r$  and  $m$ . The comparison in the above cases is found to be in excellent agreement, as shown in Table 1. The excellent agreement is an encouragement for fur-

ther study of the effects of other parameters on the dimensionless governing equations representing UCM fluid flow over a melting surface.

### 4. DISCUSSION OF RESULTS

The numerical computations have been carried out for various values of temperature dependent viscous parameter, Stratification parameter, Deborah number, Magnetic field parameter, temperature dependent thermal conductivity parameter, Prandtl number, Space dependent heat source parameter, Intensity of heat distribution on space parameter and melting parameter using numerical scheme discussed in the previous section. To avoid any corresponding effect(s) on the fluid flow (i.e. decrease in the volume and changing of state) of UCM due to high temperature when investigating the effect of dimensionless temperature dependent viscous and thermal conductivity parameters, variable  $a_1 = a_2$  in Eq. (16) may be considered as unity. In order to illustrate the results graphically, the numerical values are plotted in Figs 2 - 13.

From Table 1, it is observed that the magnitude of  $-\theta'(0)$  which is proportional to local heat transfer is small when  $m = 0$  and large when  $m = 0.5$  as Prandtl number increases. This result shows a significant increase in local heat transfer rate with an increase in melting rate. In real life, melting is a phase transformation process that is accompanied by absorption of thermal energy. Hence, this accounts for the absorption of thermal energy at the wall which corresponds to an increase in the rate of heat trans-

**Table 1 Comparison of  $f''(0)$  and  $-\theta'(0)$  using Runge-Kutta together with shooting techniques and `bvp4c` with  $P_r$  and  $m$  when  $\eta_\infty = 6$**

	$f''(0)$ RK4SM	$f''(0)$ <code>bvp4c</code>
$P_r = 0.3, m = 0$	0.0223028	0.022302813
$P_r = 0.4, m = 0$	0.0223028	0.022302813
$P_r = 0.5, m = 0$	0.0223028	0.022302813
$P_r = 0.7, m = 0$	0.0223028	0.022302813
$P_r = 0.3, m = 0.5$	0.0146914	0.014691075
$P_r = 0.4, m = 0.5$	0.0171746	0.017174749
$P_r = 0.5, m = 0.5$	0.0187310	0.018731087
$P_r = 0.7, m = 0.5$	0.0204998	0.020499887
	$-\theta'(0)$ RK4SM	$-\theta'(0)$ <code>bvp4c</code>
$P_r = 0.3, m = 0$	-0.0716716	-0.071671675
$P_r = 0.4, m = 0$	-0.0606259	-0.060625997
$P_r = 0.5, m = 0$	-0.0508994	-0.050899542
$P_r = 0.7, m = 0$	-0.0344803	-0.034480445
$P_r = 0.3, m = 0.5$	-0.0683261	-0.068325631
$P_r = 0.4, m = 0.5$	-0.0581836	-0.058183585
$P_r = 0.5, m = 0.5$	-0.0491345	-0.049134832
$P_r = 0.7, m = 0.5$	-0.0336167	-0.033616759

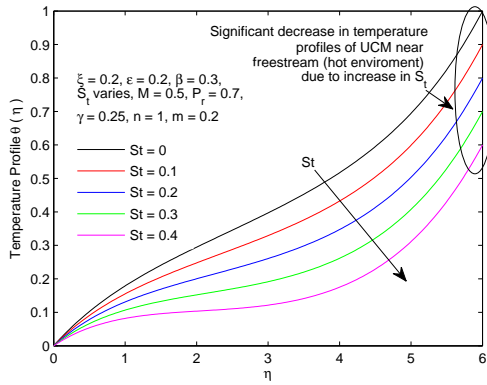


**Fig. 2. Temperature profiles  $\theta(\eta)$  for different values of stratification parameter ( $S_t$ ).**

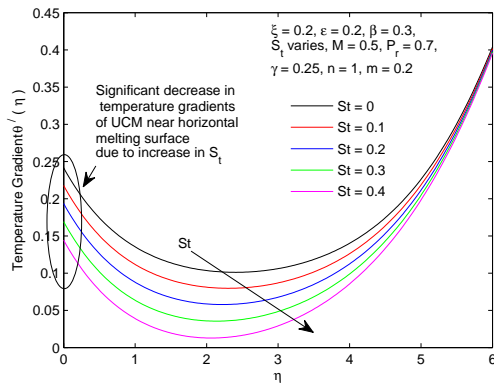


**Fig. 3. Temperature Gradient profiles  $\theta'(\eta)$  for different values of stratification parameter ( $S_t$ ).**

fer with melting. This result is in good agreement with the report of Fukusako and Yamada (1999). The variations of temperature profiles  $\theta(\eta)$  along similarity variable  $\eta$  with different values of stratification parameter are plotted in Fig. 2. At a constant value of stratification parameter, it is seen that  $\theta(\eta)$  enlarges continuously as  $\eta$  grows. At all points in the fluid domain ( $0 \leq \eta \leq 6$ ), it is seen that  $\theta(\eta)$  decreases with an increase in the magnitude of stratification parameter with a negligible decrease few distance from the melting surface and significant decrease thereafter till freestream. Physically, increase in the magnitude of stratification parameter corresponds to a systematic way of decreasing the heat energy from the freestream (i.e. to control the heat energy from upper hot environment into the fluid domain). It is worth mentioning that as the heat energy is reducing, hence the temperature of the UCM fluid within the fluid layer is decreasing. The negligible decrease near the melting surface shown in Fig. 2. can be traced to the rate of melting which

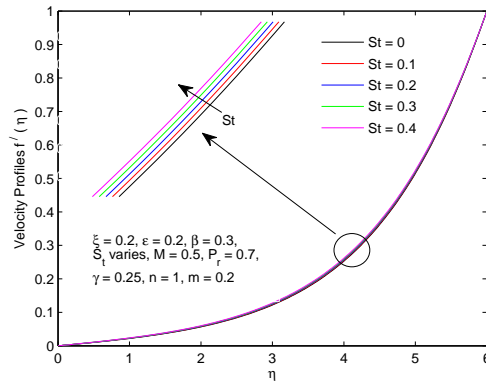


**Fig. 4. Velocity Profiles  $f'(\eta)$  for different values of stratification parameter ( $S_t$ ).**

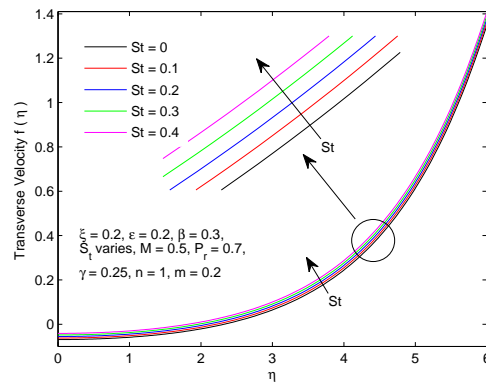


**Fig. 5. Transverse Velocity Profiles  $f(\eta)$  for different values of stratification parameter ( $S_t$ ).**

occurs at the wall (i.e.  $m = 0.2$ ). This behavior near the horizontal wall can be controlled by either increasing or decreasing the magnitude of  $m$  while increasing thermal stratification parameter. The result is in good agreement with real life situation based on the fact that a decrease in temperature is significant near freestream and decreases negligibly as  $\eta$  tends from 6 to 0. It is also noticed that this decrease obey the melting boundary condition of temperature at the wall ( $\theta_{\eta=0} = T_m = 0$ ). It is observed in Fig. 3. that temperature gradient is a decreasing function of stratification at all point of  $\eta$ . It is further seen that all profiles tend to 0.4 as  $\eta \rightarrow 6$ . From this graph, it is evidently to report that  $-\theta'(0)$  which is proportional to local heat transfer rate increases significantly with an increase in stratification. In Fig. 3, we also notice that  $-\theta'(0)$  increases negligible at the freestream with an increase in  $S_t$ . In this study, setting  $m = 0$  can seriously affect the melting processes at the wall. In addition to this fact, existence of melting at the wall together with an increase in stratification parameter depicts a negligible increase in

longitudinal velocity and significant increase in transverse velocity (see Fig. 4 and Fig. 5). As temperature decreases with an increase in stratification parameter, velocity profiles are expected to decrease as reported in Animasaun (2015a). It is worth noticing that such effect exists due to the presence of suction and the kind of fluid under consideration (Casson fluid). In this research, mathematical model which denote melting heat transfer has replaced the suction at the wall. It is also important to remark that the results we obtained here is in good agreement with that of Fig. 6. reported in Hayat *et al.* (2013). We believe that this influence requires further investigation by replacing melting heat transfer model with suction model (i. e. to study the effect of suction on UCM fluid with variable thermo-physical properties subject to thermal stratification).

It is also important to report that the influence of freestream temperature together with internally exponential heat source account for the increase in velocity and transverse velocity of UCM as it flows. Infact, these influences totally subdues the effect of increasing stratification which ought to decrease the velocity profile as reported in Animasaun (2015a). The variations of  $f(\eta)$  along  $\eta$  with different values of  $\xi$  are plotted in Fig. 6. It is seen that the increase of  $\xi$  leads to the enhancement of the velocity profiles. We further notice that, increase in the magnitude of  $\xi$  has no effect on  $f(\eta)$  near the melting wall. As shown in Fig. 6,  $\xi$  has an evident effect on  $f(\eta)$  that the larger the value of  $\xi$  is, the greater the velocity is. The physics behind this is that, as magnitude of  $\xi$  increases at a constant value of  $b_1$ , this corresponds to an increase in temperature difference of  $(T_\infty - T_o)$ . Hence, this increase in temperature weakens the intermolecular forces which hold the molecule of UCM so tight. In view of this, the dynamic viscosity is gradually reduced and corresponds to increase in velocity as shown in Fig. 6 and Fig. 7. It is further observed in Fig. 7. that increase in the magnitude of temperature dependent viscous parameter has negligible effect on velocity profiles near the free stream. Physically, the temperature of UCM near the hot environment (free stream) is almost the same. In such a situation, the flow velocity approaches to the maximum value. In this study, it is important to note that increase in the temperature dependent thermal conductivity parameter ( $\epsilon$ ) at a constant value of  $b_2$  corresponds to an increase in temperature difference  $(T_\infty - T_o)$ . This explains the increase in temperature profiles shown in Fig. 8. due to increase in the magnitude of  $\epsilon$ .

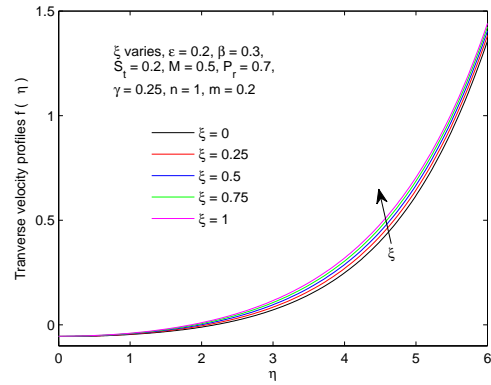


**Fig. 6. Transverse Velocity Profiles  $f(\eta)$  for different values of temperature dependent viscous conductivity parameter ( $\xi$ ) when  $\epsilon = 0.2, m = 0.2$ .**

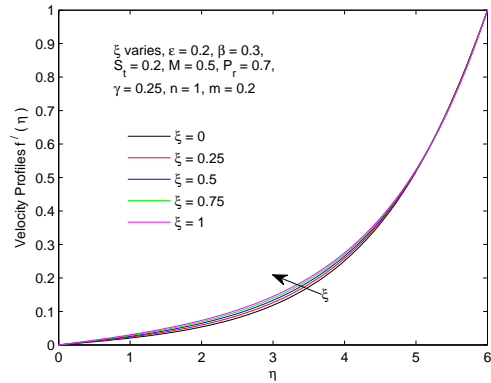


**Fig. 7. Velocity Profiles  $f'(\eta)$  for different values of temperature dependent viscous conductivity parameter ( $\xi$ ) when  $\epsilon = 0.2, m = 0.2$ .**

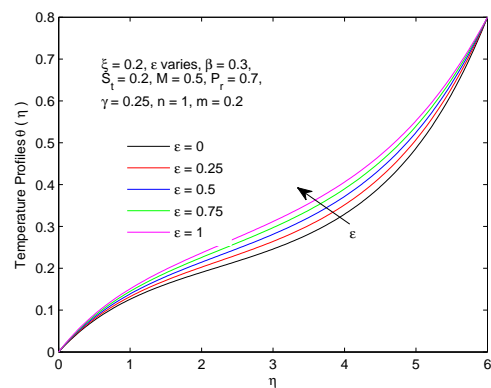


**Fig. 8. Temperature Profiles  $\theta(\eta)$  for different values of temperature dependent thermal conductivity parameter ( $\epsilon$ ) when  $\xi = 0.2, \gamma = 0.25$ .**

In the absence of melting heat transfer, thermal stratification and energy equation, Eq. (24) - Eq. (27) reduces to the fluid flow problem con-

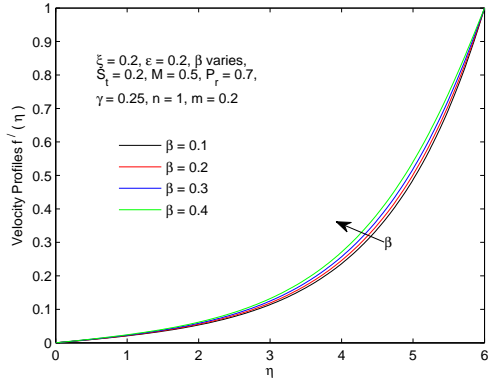


**Fig. 9. Velocity Profiles  $f'(\eta)$  for different values of Deborah number ( $\beta$ ) when  $\xi = \epsilon = 0.2$ .**

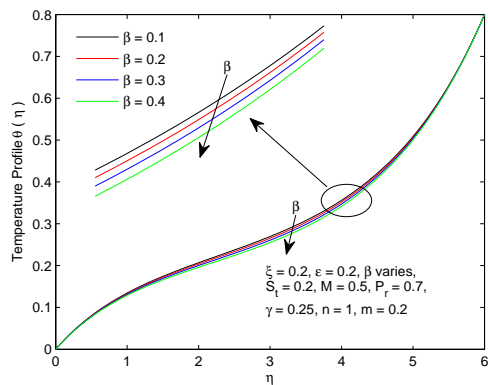


**Fig. 10. Temperature Profiles Profiles  $\theta(\eta)$  for different values of Deborah number ( $\beta$ ) when  $\xi = \epsilon = 0.2$ .**

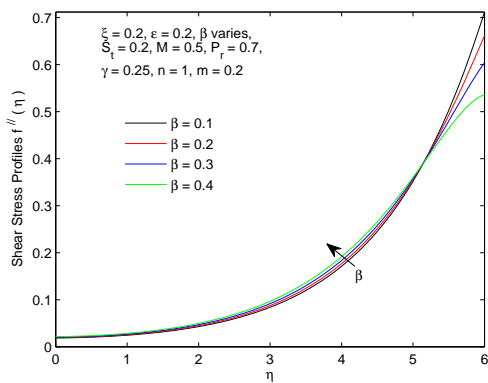


**Fig. 11. Shear stress Profiles  $f''(\eta)$  for different values of Deborah number ( $\beta$ ) when  $\xi = \epsilon = 0.2$ .**

considered by Motsa *et al.* (2012) if  $f'(0) = 1$ ,  $f(0) = R = 0$  and  $f'(\eta \rightarrow \infty) = 0$  where  $R$  is defined as suction parameter. In this limiting case, increase in the magnitude of Deborah number corresponds to decrease in velocity profiles. Physically, this result is true. At a con-

stant value of stretching rate (with S.I. unit  $s^{-1}$ ), increase in the magnitude of Deborah number implies increase in relaxation time; hence, the UCM fluid behaves like a solid as it flows. This account for the decrease in velocity profiles. It is worth mentioning that this result holds due to the stretching at the wall. In view of this, no-slip condition ( $u = 0$  at  $y = 0$ ) tends to have a great influence on the effect of increasing Deborah number on velocity profile of UCM. To unravel the dynamics of UCM fluid flow over melting surface towards hot environment, it is valid to consider (i)  $T(y = 0) = T_m$  which leads to  $\theta(\eta = 0) = 0$ , (ii)  $T(y \rightarrow \infty) \rightarrow T_\infty$  which leads to  $\theta(\eta \rightarrow \infty) \rightarrow (1 - S_t)$ , (iii)  $u(y = 0) = 0$  which leads to  $f'(\eta) = 0$ , and (iv)  $u(y \rightarrow \infty) \rightarrow u_e$  which leads to  $f'(\eta) \rightarrow 1$ . All these facts account for the increase in velocity function with Deborah number as shown in 9. We then examine the effects of Deborah number on the profiles of temperature and shear stress. It is observed in Fig. 10. that temperature profiles decreases with an increase in the magnitude of Deborah number within the fluid domain. It is shown in Fig. 11. that shear stress of UCM decreases very close to the free stream with an increase in Deborah number.

Fig. 12. and Fig. 13. illustrates the effects of Deborah number and melting heat transfer rate on local skin friction coefficient and local heat transfer rate. At a constant value of Deborah number, the local skin friction coefficient reduces significantly with an increase in melting rate. Physically, increase in melting rate absorbed all heat energy near the wall and this enhance drag. The same effect is observed when the magnitude of Deborah number is increased. It is further observed that the rate at which lo-

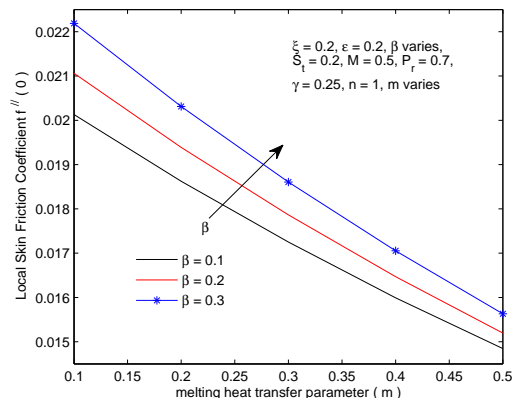


**Fig. 12. Variation of the local skin friction coefficient with melting parameter ( $m$ ) and Deborah number ( $\beta$ ).**

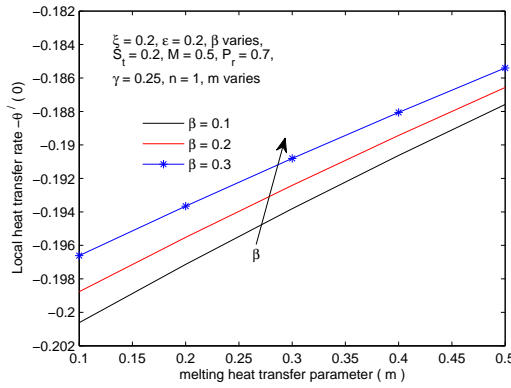


**Fig. 13. Variation of the local heat transfer rate with melting parameter( $m$ ) and Deborah number ( $\beta$ ).**

cal skin friction decreases with melting is low at small magnitude of  $\beta$  and high at large magnitude of  $\beta$ . In Fig. 13, it is shown that  $-\theta'(\eta)$  which is proportional to local heat transfer rate increases with melting heat transfer rate and also increases with an increase in the magnitude of Deborah number. The values of  $f(0)$ ,  $f'(0)$  and  $-\theta'(0)$  for different values of  $m$  and  $\beta$  are listed in Table 2 - 4. It is seen that at a constant value of  $\beta$ , transverse velocity at the wall ( $\eta = 0$ ) decreases with  $m$  (see Table 2). It is

**Table 2 Values of Transverse velocity at the wall  $f(0)$  for different values of melting parameter  $m$  when  $\xi = \epsilon = S_t = 0.2$ ,  $\beta$  varies,  $M = 0.5$ ,  $P_r = 0.7$ ,  $\gamma = 0.25$ ,  $n = 1$  and  $m$  varies when  $\eta_\infty = 6$**

	$f(0)$ $\beta = 0.1$	$f(0)$ $\beta = 0.3$
$m = 0.1$	-0.028659690	-0.028087040
$m = 0.2$	-0.056323955	-0.055329768
$m = 0.3$	-0.083061375	-0.081774033
$m = 0.4$	-0.108928104	-0.107462729
$m = 0.5$	-0.133987521	-0.132428171

**Table 3 Values of Transverse velocity at the wall  $f''(0)$  for different values of melting parameter  $m$  when  $\xi = \epsilon = S_t = 0.2$ ,  $\beta$  varies,  $M = 0.5$ ,  $P_r = 0.7$ ,  $\gamma = 0.25$ ,  $n = 1$  and  $m$  varies when  $\eta_\infty = 6$**

	$f''(0)$ $\beta = 0.1$	$f''(0)$ $\beta = 0.3$
$m = 0.1$	0.0201296768	0.0221872933
$m = 0.2$	0.0186232546	0.0203127802
$m = 0.3$	0.0172505593	0.0186068275
$m = 0.4$	0.0159924637	0.0170528754
$m = 0.5$	0.0148444582	0.0156300600

**Table 4 Values of local heat transfer rate at the wall  $-\theta'(0)$  for different values of melting parameter  $m$  when  $\xi = \epsilon = S_t = 0.2$ ,  $\beta$  varies,  $M = 0.5$ ,  $P_r = 0.7$ ,  $\gamma = 0.25$ ,  $n = 1$  and  $m$  varies when  $\eta_\infty = 6$**

	$-\theta'(0)$ $\beta = 0.1$	$-\theta'(0)$ $\beta = 0.3$
$m = 0.1$	-0.200617833	-0.196609283
$m = 0.2$	-0.197133845	-0.193654188
$m = 0.3$	-0.193809875	-0.190806077
$m = 0.4$	-0.190624182	-0.188059777
$m = 0.5$	-0.187582530	-0.185399439

further observed in Table 2 that at high value of melting (i.e.  $m = 0.5$ ), the magnitude of  $f(0)$  when  $\beta = 0.3$  is greater than when  $\beta = 0.1$ .

### 5. CONCLUSION

We have numerically studied the similarity solutions of steady upper-convected Maxwell fluid flow over melting surface situated in hot environment. The corresponding influences of thermal stratification, variation in viscosity and thermal conductivity due to temperature are properly considered. The governing (dimensional) partial differential equations are converted into (dimensionless) nonlinear ordinary differential equations by using similarity transformation. Mathematical expressions which can be used to investigate the effects of temperature on the viscosity of UCM at the melting wall and near the freestream is presented. The dimensionless governing equations are solve numerically. Results for the skin friction coefficient, local Nusselt number, transverse velocity profiles, velocity profiles as well as temperature profiles are presented for different values of the governing parameters. Effects of the melting parameter, temperature dependent viscous parameter, temperature dependent thermal conductivity parameter, Deborah number and Prandtl number on the flow and heat transfer characteristics are thoroughly examined. The main points of the present study can be summed up as follows:

- Longitudinal velocity and transverse velocity are increasing functions of stratification parameter. The classical effect of increasing stratification on velocity is subdued by the intense freestream temperature together with internal exponentially heat source.
- At small magnitude of Deborah number within ( $0.1 \leq \beta \leq 0.3$ ), local skin friction coefficient decreases significantly with an

increase in melting. The local skin friction coefficient increases significantly with an increase in Deborah number at large magnitude of melting parameter and increases more significantly at small magnitude of melting parameter. The magnitude of transverse velocity at the wall  $f(0)$  when  $\beta = 0.3$  is larger than when  $\beta = 0.1$ . Within small range of melting heat transfer (i.e.  $0.1 \leq m \leq 0.2$ ), decrease in local skin friction is more pronounced when magnitude of Deborah number is very large.

- At a constant value of Deborah number, local heat transfer rate decreases with melting heat transfer. At each value of melting parameter within ( $0.1 \leq m \leq 0.5$ ), local heat transfer rate increases with Deborah number.
- As UCM fluid experiencing deformation over a given time frame, the behavior (dynamic) of UCM is strongly dependent on the stretching at the wall. Increase in Deborah number corresponds to an increase in velocity profiles provided  $u(x, y = 0) = 0$  and  $u(x, y \rightarrow 0) \rightarrow u_e$  (Blasius Boundary Condition).

#### ACKNOWLEDGMENTS

The authors wish to express their thanks to the anonymous Reviewer for his/her valuable and interesting comments.

#### REFERENCES

- Abbas, Z., T. Hayat, and N. Alib (2008). Mhd flow and mass transfer of a upper-convected maxwell fluid past a porous shrinking sheet with chemical reaction species. *Physics Letters A* 372(26), 4698–4704.
- Abbas, Z., M. Sajid, and T. Hayat (2006). Mhd boundary-layer flow of an upper-convected maxwell fluid in a porous channel. *Theoretical and Computational Fluid Dynamics* 20(4), 229–238.
- Animasaun, I. L. (2015a). Casson fluid flow of variable viscosity and thermal conductivity along exponentially stretching sheet embedded in a thermally stratified medium with exponentially heat generation. *Journal of Heat and Mass Transfer Research* 2(2), Article in Press.
- Animasaun, I. L. (2015b). Effects of thermophoresis, variable viscosity and thermal conductivity on free convective heat and mass transfer of non-darcian mhd dissipative casson fluid flow with suction and nth order of chemical reaction. *Journal of the Nigerian Mathematical Society-Elsevier* 34, 11–31.
- Animasaun, I. L., E. Adebile, and A. Fagbade (2015). Casson fluid flow with variable thermo-physical property along exponentially stretching sheet with suction and exponentially decaying internal heat generation using the homotopy analysis method. *Journal of the Nigerian Mathematical Society*.
- Animasaun, I. L., K. S. Adegbe, A. J. Omowaye, and A. B. Disu (2015). Heat and mass transfer of upper convected maxwell fluid flow with variable thermo-physical properties over horizontal melting surface. *Applied Mathematics* 6(-), 1362-1379.
- Barnes, H. A., J. F. Hutton, and K. Walters (1989). *An Introduction to Rheology*. New York: Elsevier Science Publishing Company.
- Batchelor, G. K. (1987). *An Introduction to Fluid Dynamics*. London: Cambridge University Press.
- Charraudeau, J. (1975). Influence de gradients de propriétés physiques en convection force application au cas du tube. *International Journal of Heat and Mass Transfer* 18(1), 87–95.
- Crepeau, J. and R. Clarksean (1997). Similarity solutions of natural convection with internal heat generation. *Transactions of ASME - Journal of Heat Transfer* (119), 184–185.
- Dunn, J. and K. Rajagopal (1995). Fluids of differential type: critical review and thermodynamic analysis. *International Journal of Engineering Science* 33(5), 689–729.
- Epstein, M. (1975). The effect of melting on heat transfer to submerged bodies. *Letters in Heat and Mass Transfer* 2(2), 97–104.
- Epstein, M. and D. H. Cho (1976). Melting heat transfer in steady laminar flow over a flat plate. *Journal of Heat Transfer* 98, 531–533.
- Fosdick, R. L. and K. R. Rajagopal (1979). Anomalous features in the model of second grade fluids. *Archive for Rational Mechanics and Analysis* 70(2), 145–152.

- Fukusako, S. and M. Yamada (1999). Melting heat transfer inside ducts and over external bodies. *Experimental Thermal and Fluid science* 19(2), 93–117.
- Hayat, T., Z. Abbas, and M. Sajid (2006). Series solution for the upper-convected maxwell fluid over a porous stretching plate. *Physics Letters A* (358), 396–403.
- Hayat, T., M. Hussain, M. Awais, and S. Obaidat (2013). Melting heat transfer in a boundary layer flow of a second grade fluid under sores and dufour effects. *International Journal of Numerical Methods for Heat and Fluid Flow* 23, 1155–1168.
- Hayat, T., S. A. Shehzad, H. H. Al-Sulami, and S. Asghar (2013). Influence of thermal stratification on the radiative flow of maxwell fluid. *Journal of the Brazilian Society of Mechanical Sciences and Engineering* 35(4), 381–389.
- Ishak, A., R. Nazar, N. Bachok, and I. Pop (2010). Melting heat transfer in steady laminar flow over a moving surface. *Heat Mass Transfer* (46), 463–468.
- Larson, R. (1988). *Constitutive Equations for Polymer Melts and Solutions*. Boston: Butterworths.
- Lienhard-IV, J. H. and J. H. Lienhard-V (2008). *A heat Transfer Textbook, 3rd Edition*. Cambridge, Massachusetts, U.S.A.: Phlogiston Press.
- Meyers, T. G., J. Charpin, and M. Tshela (2006). The flow of a variable viscosity fluid between parallel plates with shear heating. *Applied Mathematic Modelling* 30(9), 799–815.
- Motsa, S., T. Hayat, and O. M. Aldossary (2012). Mhd flow of upper-convected maxwell fluid over porous stretching sheet using successive taylor series linearization method. *Applied Mathematics and Mechanics (English Edition)* 33(8), 975–990.
- Mukhopadhyay, S. (2013). Effects of thermal radiation and variable fluid viscosity on stagnation point flow past a porous stretching sheet. *Meccanica-Springer* 48, 1717–1730 <http://dx.doi.org/10.1007/s11012-013-9704-0>.
- Mustafa, M., T. Hayat, S. A. Shehzad, and S. Obaidat (2012). Melting heat transfer in the stagnation-point flow of an upper-convected maxwell (ucm) fluid past a stretching sheet. *International Journal for Numerical Methods in Fluids* 68(2), 233–243.
- Na, T. Y. (1979). *Computational Methods in Engineering Boundary Value Problems*. New York: Academic Press.
- Poole, R. J. (2012). The Deborah and Weissenberg numbers. *Rheology Bulletin* 53(2), 32–39.
- Pop, I., N. Bachok, and A. Ishak (2010). Melting heat transfer in boundary layer stagnation-point flow towards a stretching/shrinking sheet. *Physics Letter A* 374(4), 4075–4079.
- Pop, I., A. Sujatha, K. Vajravelu, and K. Prasad (2012). Mhd flow and heat transfer of a ucm fluid over a stretching surface with variable thermophysical properties. *Meccanica-Springer* 47(6), 1425–1439.
- Prasad, K., K. Vajravelu, and A. Sujatha (2013). Influence of internal heat generation/absorption, thermal radiation, magnetic field, variable fluid property and viscous dissipation on heat transfer characteristics of a maxwell fluid over a stretching sheet. *Journal of Applied Fluid Mechanics* 6(2), 249–256.
- Reddy, M. G. and N. B. Reddy (2011). Mass transfer and heat generation effects on mhd free convection flow past an inclined vertical surface in a porous medium. *Journal of Applied Fluid Mechanics* 4(2), 7–11.
- Sadeghy, K., V. Aliakbar, and A. Alizadeh-Pahlavan (2009). The influence of thermal radiation on mhd flow of maxwellian fluids above stretching sheets. *Communications in Nonlinear Science and Numerical Simulation* 14(3), 779–794.
- Sadeghy, K., H. Hajibeygi, and S. M. Taghavi (2006). Stagnation-point flow of upper-convected maxwell fluids. *International Journal of Non-Linear Mechanics* 41(10), 1242 – 1247.
- Sadeghy, K., A. H. Najafi, and M. Safaripour (2005). Sakiadis flow of an upper-convected maxwell fluid. *International Journal of Non-Linear Mechanics* 40(9), 1220 – 1228.
- Salem, A. M. and M. A. El-Aziz (2007). Mhd-mixed convection and mass transfer from a vertical stretching sheet with diffusion of chemically reactive

- species and space- or temperature-dependent heat source. *Canadian Journal of Physics* 85(4), 359–373.
- Salem, A. M. and M. A. El-Aziz (2008). Effect of hall currents and chemical reaction on hydromagnetic flow of a stretching vertical surface with internal heat generation/absorption. *Applied Mathematical Modelling* 32(7), 1236–1254.
- Schlichting, H. (1964). *Boundary Layer Theory, Sixth Edition*. New York: McGraw-Hill.
- Shampine, L. F., M. W. Reichelt, and J. Kierzenka (2010). Solving boundary value problems for ordinary differential equations in matlab with bvp4c. pp. Available at <http://www.mathworks.com/bvptutorial>.
- Shateyi, S., S. S. Motsa, and Z. Makukula (2015). On spectral relaxation method for entropy generation on a mhd flow and heat transfer of a maxwell fluid. *Journal of Applied Fluid Mechanics* 8(1), 21–31.
- Sivagnana, K. K. P., R. Kandasamy, and R. Saravanan (2009). Lie group analysis for the effect of viscosity and thermophoresis particle deposition on free convective heat and mass transfer in the presence of suction / injection. *Theoretical and Applied Mechanics* 36(4), 275–298.
- Tien, C. and Y. Yen (1965). The effect of melting on forced convection heat transfer. *Journal of Applied Meteorology* 4(4), 523–527.
- Vimala, C. and P. Loganathan (2015). Mhd flow of nanofluids over an exponentially stretching sheet embedded in a stratified medium with suction and radiation effects. *Journal of Applied Fluid Mechanics* 8(1), 85–93.
- Yin-Chao, Y. and C. Tien (1963). Laminar heat transfer over a melting plate, the modified leveque problem. *Journal of Geophysical Research* 68(12), 3673–3678.